









Contrasting effector profiles between bacterial colonisers of kiwifruit reveal redundant roles converging on PTI-suppression and RIN4

Jay Jayaraman¹ , Minsoo Yoon¹ , Lauren M. Hemara^{1,2} , Deborah Bohne¹, Jibrán Tahir¹ , Ronan K. Y. Chen³ , Cyril Brendolise¹ , Erik H. A. Rikkerink¹  and Matthew D. Templeton^{1,2,4} 

¹The New Zealand Institute for Plant and Food Research Ltd, Mt. Albert Research Centre, Auckland 1025, New Zealand; ²School of Biological Sciences, University of Auckland, Auckland 1010, New Zealand; ³The New Zealand Institute for Plant and Food Research Ltd, Food Industry Science Centre, Palmerston North 4472, New Zealand; ⁴Bioprotection Aotearoa, Lincoln 7647, New Zealand

Summary

Authors for correspondence:

Matthew D. Templeton

Email: matt.templeton@plantandfood.co.nz

Jay Jayaraman

Email: jay.jayaraman@plantandfood.co.nz

Received: 10 November 2022

Accepted: 14 February 2023

New Phytologist (2023) 238: 1605–1619
doi: 10.1111/nph.18848

Key words: effectors, pathogenesis, plant pathogen, *Pseudomonas syringae*, type III secretion system, virulence.

- Testing effector knockout strains of the *Pseudomonas syringae* pv. *actinidiae* biovar 3 (Psa3) for reduced *in planta* growth in their native kiwifruit host revealed a number of nonredundant effectors that contribute to Psa3 virulence. Conversely, complementation in the weak kiwifruit pathogen *P. syringae* pv. *actinidifoliorum* (Pfm) for increased growth identified redundant Psa3 effectors.
- Psa3 effectors hopAZ1a and HopS2b and the entire exchangeable effector locus (Δ EEL; 10 effectors) were significant contributors to bacterial colonisation of the host and were additive in their effects on virulence. Four of the EEL effectors (HopD1a, AvrB2b, HopAW1a and HopD2a) redundantly contribute to virulence through suppression of pattern-triggered immunity (PTI).
- Important Psa3 effectors include several redundantly required effectors early in the infection process (HopZ5a, HopH1a, AvrPto1b, AvrRpm1a and HopF1e). These largely target the plant immunity hub, RIN4.
- This comprehensive effector profiling revealed that Psa3 carries robust effector redundancy for a large portion of its effectors, covering a few functions critical to disease.

Introduction

Bacterial pathogens of plants deploy proteinaceous effectors via their type III secretion system (T3SS) to manipulate their plant hosts and facilitate disease. The *Pseudomonas syringae* species complex delivers as many as 50 secreted effectors to suppress host immunity, as well as to extract nutrients and water from host cells into the apoplastic space (Xin *et al.*, 2016; Gentzel *et al.*, 2022; Roussin-Léveillé *et al.*, 2022). Redundancy within each *P. syringae* strain's effector repertoire confounds our ability to discern whether particular mechanisms of plant manipulation are universal or host-specific. To date, only the Arabidopsis and tomato pathogen *P. syringae* pv. *tomato* DC3000 (Pto DC3000) has been extensively and comprehensively studied for effector contributions to host infection. Extensive studies in the model plant *Nicotiana benthamiana*, which can also be infected by DC3000 variants, have been particularly important for understanding effector roles in host manipulation (Kvitko *et al.*, 2009; Cunnac *et al.*, 2011; Wei *et al.*, 2015, 2018). However, with largely a single point of pathogen reference, understanding how plant pathogens like *P. syringae* can manipulate many different host plants is challenging.

How pathogens and weak/nonpathogens differ in their colonisation of various host plants is also unclear. The mechanisms of growth within plant hosts for bacterial plant pathogens vs those deployed by the myriad of largely epiphytic commensal bacterial species have only recently been investigated (Chen *et al.*, 2020; Velásquez *et al.*, 2022). Notably, epiphytic commensal bacteria, much like avirulent pathogenic bacteria that trigger plant immunity, appear to grow only to low but stable numbers *in planta* and display a stationary phase-like growth–death balance (Velásquez *et al.*, 2022). A significant proportion of epiphytic commensals, environmentally isolated bacteria and even symbiotic bacteria possess a functional T3SS but cause little to no disease; thus, the role of a T3SS in these species is unclear (Diallo *et al.*, 2012; Tampakaki, 2014; Levy *et al.*, 2018). The notion of what constitutes a pathogen, including different strategies of colonisation success, may also limit our understanding of the evolution of plant–pathogen relationships (particularly in nature on diverse wild genotypes, as opposed to large human-manipulated plant monocultures). The lessons behind what makes a pathogen vs a commensal strain are critical to understanding how pathogens emerge and what drives their adaptation to cause virulent disease.

The molecular mechanism of plant immunity is currently understood to be comprised of two broad layers: defence at the cell membrane and intracellular defence. Defence at the plant cell membrane is mediated by transmembrane pattern recognition receptor (PRR) proteins, which recognise evolutionarily conserved pathogen-associated molecular patterns (PAMPs), triggering pattern-triggered immunity (PTI; DeFalco & Zipfel, 2021). PTI involves a series of plant responses including defence gene expression, hormonal fluxes, apoplastic reactive oxygen species production and a characteristic callose deposition within the apoplast to block the pathogen incursion (Boller & Felix, 2009; Luna *et al.*, 2011). A successful pathogen will overcome PTI through effector deployment. In response to effector presence, plants may deploy their second layer of defence, called effector-triggered immunity (ETI), which is a potentiation and strengthening of PTI responses (Ngou *et al.*, 2021; Yuan *et al.*, 2021). ETI is triggered intracellularly and is often dependent on effector recognition by polymorphic nucleotide-binding site leucine-rich repeat (NLR) proteins, either directly by binding to effectors or indirectly through sensing effector presence on guarded proteins – guardees. Often these guardees are protein hubs of PTI or ETI. RPM1-interacting protein 4 (RIN4) is one such immunity hub, is guarded by evolutionarily unlinked resistance proteins in different plants and is targeted by many different bacterial pathogens (Mackey *et al.*, 2002, 2003; Wilton *et al.*, 2010; Mazo-Molina *et al.*, 2019; Prokchorchik *et al.*, 2020; Choi *et al.*, 2021).

The kiwifruit bacterial canker pathogen *P. syringae* pv. *actinidiae* (Psa) is a new but growing focus of study for bacterial pathogenesis, in its relationship with its perennial host plant, kiwifruit. Effectors AvrE1d and HopR1b from the particularly virulent Psa biovar 3 (Psa3) have been associated with strong nonredundant contributions to kiwifruit infection (Jayaraman *et al.*, 2020). A closely related ubiquitous epiphytic commensal/weak pathogen of kiwifruit, *P. syringae* pv. *actinidifoliorum* (Pfm), has also been described with a functional T3SS and the ability to cause disease on non-kiwifruit plants (Cunty *et al.*, 2015; Ferrante & Scortichini, 2015). While several different genetic components have been proposed to be important in woody plant pathogens, Pfm, unlike other epiphytic kiwifruit bacterial colonisers, has all the hallmarks of a successful kiwifruit pathogen: a functional T3SS, a reasonably large repertoire of effectors and the catechol/ β -ketoacid pathway (Bartoli *et al.*, 2015; Nowell *et al.*, 2016; Templeton *et al.*, 2022). The contrast between Psa3 and Pfm offers an interesting opportunity to study the parameters involved in severe disease outbreaks on plant monocultures, with particular focus on effectors.

Materials and Methods

Bioinformatics and sequence analyses

Genome sequences for Psa3 ICMP 18884 (Psa3 V-13; CP011972-3) and Pfm ICMP 18804 (Pfm LV-5; CP081457) were obtained from NCBI GenBank. The Psa3 V-13 and Pfm LV-5 genomes were annotated previously (Templeton *et al.*, 2015, 2022). Sequences for type III secreted effectors (T3Es) from Psa3 V-13 and Pfm LV-5 were analysed on GENEIOUS R11 software (<https://www.geneious.com>; Biomatters, Auckland, New Zealand) with built-in GENEIOUS DNA and amino acid sequence alignments, tree building and annotation tools. Effector protein structures were predicted using ALPHAFOLD2 v.2.2.0 with a max_template_date of 2022-1-1 (Jumper *et al.*, 2021).

<https://www.geneious.com>; Biomatters, Auckland, New Zealand) with built-in GENEIOUS DNA and amino acid sequence alignments, tree building and annotation tools. Effector protein structures were predicted using ALPHAFOLD2 v.2.2.0 with a max_template_date of 2022-1-1 (Jumper *et al.*, 2021).

Bacterial strains and growth conditions

The bacterial strains and plasmids used in this study are listed in Supporting Information Table S1. Psa3 V-13 and Pfm LV-5 strains were grown in lysogeny broth (LB), supplemented with nitrofurantoin and cephalexin, at 20°C with shaking at 200 rpm. *Escherichia coli* strains were grown in LB with appropriate antibiotics at 37°C. The concentrations of antibiotics used in selective media were kanamycin 50 $\mu\text{g ml}^{-1}$, gentamicin 25 $\mu\text{g ml}^{-1}$, nitrofurantoin 12.5 $\mu\text{g ml}^{-1}$ and cephalexin 40 $\mu\text{g ml}^{-1}$ (all from Sigma-Aldrich). Plasmids were transformed into electrocompetent Psa3 (Mesarich *et al.*, 2017) or *E. coli* by electroporation using a Bio-Rad Gene Pulser Xcell and recovered for 1 h in LB before plating on selective media.

Effector knockout

To make the Pfm LV-5 ΔhopA1a , ΔhopE1a , or $\Delta\text{hopA1a}/\Delta\text{hopE1a}$ mutants, or Psa3 V-13 ΔhopH1a , $\Delta\text{hopQ1a}/\Delta\text{hopD1a}$, $\Delta\text{hopS2b}/\Delta\text{hopAZ1a}$, $\Delta\text{CEL}/\Delta\text{x}EEL$, $\Delta\text{CEL}/\Delta\text{hopS2b}/\Delta\text{hopAZ1a}$, $\Delta\text{CEL}/\Delta\text{x}EEL/\Delta\text{hopS2b}/\Delta\text{hopAZ1a}$, $\Delta\text{hopH1a}/\Delta\text{hopZ5a}/\Delta\text{avrPto1b}$, $\Delta\text{hopH1a}/\Delta\text{hopZ5a}/\Delta\text{avrPto1b}/\Delta\text{avrRpm1a}$ and $\Delta\text{hopH1a}/\Delta\text{hopZ5a}/\Delta\text{avrPto1b}/\Delta\text{avrRpm1a}/\Delta\text{tEEL}$ mutants, methodologies similar to that used for Psa3 V-13 multieffector knockouts described earlier were used (Hemara *et al.*, 2022). Briefly, for each multieffector knockout, a selected Psa3 V-13 or Pfm LV-5 strain was transformed by electroporation with the relevant p Δ (T3E) construct and transconjugants were selected on LB plates with nitrofurantoin, cephalexin and kanamycin. Selected colonies were subsequently streaked onto LB plates containing 10% (w/v) sucrose to counterselect plasmid integration. Effector mutants were screened using colony PCR with primers Psa_(T3E)-KO_Check-F and Psa_(T3E)-KO_Check-R and sent for Sanger sequencing with the cloning Psa_(T3E)-KO_UP-F and Psa_(T3E)-KO_DN-R primers described earlier (Hemara *et al.*, 2022). Mutants were also confirmed by plating on kanamycin-containing medium to confirm the loss of the integrated *nptII* gene (and associated *sacB* gene).

Effector plasmid complementation

For native-promoter constructs of Pfm LV-5 effectors, the full region including the HrpL box promoter was PCR-amplified using primers (Table S2) and Q5 High-Fidelity DNA Polymerase (NEB, Ipswich, MA, USA). The resulting PCR fragment was gel-purified and was blunt-end-ligated into the *Eco53kI* (NEB) site of broad-host-range vector pBBR1MCS-5 (Kovach *et al.*, 1995). Constructs were transformed into *E. coli* DH5 α , plated on X-gal/IPTG-containing (for blue/white selection) LB agar plates with gentamicin, and positive transformants confirmed by Sanger sequencing (Macrogen, Seoul, South Korea). Synthetic *avrRps4*

promoter constructs of HA-tagged effectors from Psa3 V-13 or Pfm LV-5 have been described previously (Jayaraman *et al.*, 2017). All constructs were transformed into relevant Psa3 or Pfm strains by electroporation, and transformants screened for the presence of effector by gene-specific colony PCR.

In planta growth and symptomology assays

Psa3 and Pfm infection assays were carried out as described previously (McAtee *et al.*, 2018). *Actinidia chinensis* var. *chinensis* 'Hort16A' plantlets, grown from axillary buds on Murashige and Skoog rooting medium without antibiotics in sterile 400-ml plastic tubs ('pottles'), were purchased from Multiflora Laboratories (Auckland, New Zealand). Plantlets were grown at 20°C under Gro-Lux fluorescent lights under long-day conditions (16 h : 8 h, light : dark) and used when the plantlets were approximately 12 wk old. Overnight LB medium cultures of Psa3 or Pfm were pelleted at 5000 g, resuspended in 10 mM MgSO₄, reconstituted at OD₆₀₀ = 0.05 (*c.* 10⁶ CFU ml⁻¹, determined by plating) in 500 ml of 10 mM MgSO₄. Surfactant Silwet L-77 (Lehle Seeds, Round Rock, TX, USA) was added to the inoculum at 0.0025% (v/v) to facilitate leaf wetting. Pottles of 'Hort16A' plantlets were flooded with the inoculum, submerging the plantlets for 3 min, drained, sealed and then incubated under plant growth conditions, as above.

In planta growth of Psa3 or Pfm strains was assayed as described previously (McAtee *et al.*, 2018). Briefly, leaf samples of four leaf discs per biological replicate, taken randomly with a 1-cm diameter cork-borer from three plants, were harvested at 2 h (day 0), day 6 and day 12 postinoculation. All four replicates per treatment per time point were taken from the same pottle. To determine Psa3/Pfm growth inside the plant, the leaf discs were surface-sterilised, placed in Eppendorf tubes containing three sterile stainless-steel ball bearings, 350 µl 10 mM MgSO₄, and macerated in a Storm 24 Bullet Blender (Next Advance, Troy, NY, USA) for two bursts of 1 min each at maximum speed. A 10-fold dilution series of the leaf homogenates was made in sterile 10 mM MgSO₄ until a dilution of 10⁻⁸ and plated as 10 µl droplets on LB medium supplemented with nitrofurantoin and cephalixin. After 2 d of incubation at 20°C, the CFU cm⁻² of leaf area was ascertained from dilutions. To observe pathogenic symptoms on the plants, infected pottles were kept up to 50 d postinoculation and photographs taken of pottles and a representative infected leaf. Infection severity was qualitatively assessed based on typical symptoms: necrotic leaf spots, chlorotic haloes, leaf death and plant death. Each of these growth assay experiments was conducted at least three times.

PTI-suppression assays

The *N. benthamiana* PTI-suppression assay (suppression of effector delivery) was adapted from that described previously (Crabill *et al.*, 2010; Le Roux *et al.*, 2015). pBBR1MCS-5 constructs of each Psa3 V-13 or Pfm LV-5 effector (Jayaraman *et al.*, 2017) were transformed by electroporation into *P. fluorescens* (Pfo) Pf0-1 (T3S) strains (Thomas *et al.*, 2009) and plated on selective media with chloramphenicol, gentamicin and tetracycline. Positive transformants were

confirmed by gene-specific colony PCR. Pf0-1(T3S) carrying empty vector or Psa3/Pfm constructs were streaked from glycerol stocks onto LB agar plates with antibiotic selection and grown for 2 d at 28°C. Bacteria were then harvested from plates, resuspended in 10 mM MgSO₄ and diluted to the required OD₆₀₀ = 0.6 (*c.* 10⁷ CFU ml⁻¹). Infiltrations were carried out on fully expanded leaves of 4- to 5-wk-old *Nicotiana benthamiana* using a blunt-end syringe on two or three leaves (replicates). Next, 12 h postinfiltration, Pto DC3000 (OD₆₀₀ = 0.03; *c.* 10⁶ CFU ml⁻¹) was infiltrated in an overlapping area of the leaves. Pto DC3000-triggered tissue collapse was scored at 3 dpi. PTI-suppression experiments were conducted in triplicate (three leaves per plant for each effector), over three independent experimental runs (three separate plants, thus a total of *n* = 9), with tissue collapse in at least 50% of infiltrations scored as suppressors of PTI.

The *A. chinensis* PTI-suppression assay (suppression of callose deposition) was adapted from that described previously (Jin & Mackey, 2017). Briefly, for observation of callose deposits, Pfo Pf0-1 (T3S) carrying either empty vector or the plasmid-borne Psa3 effector (as before) was vacuum-infiltrated into *A. chinensis* leaves from plantlets grown in tissue culture (Multiflora Laboratories) at 2–5 × 10⁷ CFU ml⁻¹ (OD₆₀₀ of 1 in sterile 10 mM MgSO₄). The infected leaves were decolorised in lactophenol solution (water 8.3%, glycerol 8.3%, lactic acid 7%, water-saturated phenol 8.3%; in ethanol v/v) and then stained with 0.01% aniline blue in 150 mM K₂HPO₄, pH 9.5 (all chemicals from Sigma-Aldrich). Callose deposits were visualised with a Nikon Ni-E upright compound UV-fluorescence microscope equipped with a digital camera under a 40× magnification and acquired images analysed using IMAGEJ software by determining the average area of a single callose deposit and then calculated callose counts based on total callose deposit area in each image.

In vitro effector expression assay

For the detection of effector expression *in vitro*, the protocols used were based on those described previously (Huynh *et al.*, 1989). Briefly, Psa3 V-13 or Pfm LV-5 strains carrying the relevant HA-tagged effector plasmid constructs (pBBR1MCS-5) were grown in LB medium with antibiotic selection overnight, pelleted at 5000 g, washed with *hrp*-inducing minimal medium (salts supplemented with 10 mM fructose) and then resuspended in *hrp*-inducing minimal medium and incubated for 6 h with shaking for *hrp* induction. Following *hrp* induction, cells were pelleted and proteins extracted by the Laemmli method (Laemmli, 1970), resolved by SDS-PAGE and, immunoblotted for the presence of the HA-tagged effector using α-HA antibody (H9658; Sigma-Aldrich) and α-HA-HRP (3F10; Roche).

Reporter eclipse assay

Freshly expanded leaves of *A. chinensis* var. *chinensis* 'Hort16A' were co-bombarded with DNA-coated gold particles carrying pRT99-GUS and pICH86988 with the effector of interest, as described in Jayaraman *et al.* (2021). Effectors were YFP-tagged and cloned under a CaMV 35 S promoter (Choi *et al.*, 2017). Briefly, for each bombardment, 5 µl of a well-mixed particle

preparation was loaded onto a syringe filter carrier and the bombardment was performed. Target leaves were held (abaxial side uppermost) under a stainless-steel mesh (100 μm) and were bombarded once. Six bombardments (biological replicates) were performed for each particle preparation on six leaves from different plants, and each experiment was carried out in triplicate (technical replicates). After bombardment, the leaves were immersed in a 20 ml suspension of *Agrobacterium tumefaciens* GV3101 (OD_{600} adjusted to 0.6) for 30 s to trigger PTI and thus increase the subsequent ETI responses, if any, after which they were transferred onto solid MS medium.

After 48 h of incubation in the light at room temperature, the leaf tissue was frozen in liquid nitrogen, ground with metal beads, and tissue powder (*c.* 300 mg) was then mixed by vigorous vortexing with 1 ml of GUS extraction buffer (Jayaraman *et al.*, 2021). The crude extract was centrifuged at 18 000 *g* for 15 min at 4°C, and the supernatant was collected. The GUS activity was determined using 100 μl of leaf extract with methylumbelliferyl- β -glucuronide as the substrate, following the method described by Hunter & Watson (2008). For each bombardment, triplicate samples (technical replicates) were assayed and expressed in terms of pmol of MU produced per minute per gram of total protein. The means and standard errors were calculated from the six biological replicates. Data were analysed by ANOVA followed by a Tukey's HSD *post hoc* test. A plant immunity-associated cell death/hypersensitive response (HR) was inferred from a reduction of GUS activity compared with empty vector. The positive control for HR and associated reduction in GUS activity was *hopA1j* from *P. syringae* pv. *syringae* 61 (Jayaraman *et al.*, 2021).

Transient expression in *Nicotiana benthamiana* and co-immunoprecipitation

Agrobacterium tumefaciens AGL1 (YFP-tagged effectors; Choi *et al.*, 2017) or GV3101 pMP90 (FLAG-tagged AcrIN4s; Yoon & Rikkerink, 2020) was freshly grown in LB with appropriate antibiotics at 28°C with shaking at 200 rpm. Cells were pelleted by centrifugation at 4000 *g* for 10 min and resuspended in infiltration buffer (10 mM MgCl_2 , 5 mM EGTA, 100 μM acetosyringone). Cell suspensions were diluted to a final OD_{600} of 0.1 and infiltrated into at least two fully expanded leaves from a single plant of 4- to 5-wk-old *N. benthamiana* plants using a needleless syringe. All *Agrobacterium*-mediated transformation experiments were performed using premixed *Agrobacterium* cultures for the stipulated effector-RIN4 combinations in a single injection for co-immunoprecipitation experiments (see below). YFP was used as a negative control for effectors.

Tissues (0.5 g per sample) were collected 2 d postinfiltration and ground to a homogeneous powder in liquid nitrogen and resuspended in 1 ml of protein extraction buffer (1 \times PBS, 1% *n*-dodecyl- β -D-maltoside or DDM (Invitrogen, Carlsbad, CA, USA), and 0.1 tablet completeTM protease inhibitor cocktail (Sigma-Aldrich) in NativePAGETM buffer (Invitrogen)). Extracted protein samples were centrifuged at 20 000 *g* for 2 min at 4°C, and the supernatant was collected for immunoprecipitation using the

μMACS GFP Isolation Kit (Miltenyi Biotec, MediRay, New Zealand). Total and immunoprecipitated proteins were resolved on a 4–12% SDS-PAGE gel. Western blots using PVDF membranes were prepared and probed using HRP-conjugated antibodies in 0.2% I-Block (Invitrogen). Detection was achieved using ECL (Amersham, GE Healthcare, Chicago, IL, USA). The antibodies used were α -FLAG (F1804; Sigma-Aldrich), α -FLAG-HRP (A8592; Sigma-Aldrich) and α -GFP (MA515256; Life Technologies).

Statistical analyses

Sample size and statistical analyses are described in each figure legend. Typically, randomly selected samples from three to four plants (biological replicates) per treatment were analysed per individual experiment, with typically three independent experimental runs conducted for each. Plants were grown within sealed sterile plastic pottles in an environmentally controlled growth room (light, temperature) to minimise unexpected environmental variation. Leaf samples of similar ages were collected and assessed randomly for each genotype. Researchers were not blinded to allocation during experiments and outcome assessment, but order of sampling between each experimental run was varied. One-way analysis of variance (ANOVA) with Welch's test for significance was used for multisample experiments with one variable, or one-way ANOVA and Tukey's honest significant difference test was used for multivariable analyses. Statistical tests are described in the figure legends. Bar graphs and box plots were generated using R and show either mean \pm SE or median, mean and 1.5 \times interquartile range, respectively.

Results

Three new effector loci contribute quantitatively and additively to Psa3 virulence

When comparing their capacity for virulence, Pfm LV-5 is clearly incapable of causing the prolific disease symptoms in 'Hort16A' that Psa3 V-13 can, despite both species being commonly recovered from kiwifruit plants in the orchard (Fig. 1a; Chapman *et al.*, 2012; McCann *et al.*, 2013; Vanneste *et al.*, 2013; Abelleira *et al.*, 2015; Cuntly *et al.*, 2015). Comparing the host plant colonisation of Pfm LV-5 to Psa3 V-13 and Psa3 V-13 carrying the avirulence effector *hopA1j* from *P. syringae* pv. *syringae* 61 indicated that Pfm LV-5 more closely resembled the avirulent strain than pathogenic wild-type (WT) Psa3 V-13 (Fig. 1b).

Previously, *avrE1d* and *hopR1b* were found to be required for virulence (disease symptoms and host colonisation) in Psa3 V-13 infection of 'Hort16A' (Jayaraman *et al.*, 2020). Pfm LV-5 carries orthologs of both AvrE1 and HopR1, and these versions share both amino acid identity and predicted protein structure to orthologs in Psa3 V-13 (Fig. S1; Table S3). From their predicted structures, both AvrE1d and HopR1b appear to function nonredundantly as putative pore-forming effectors, a role possibly shared by HopAS1b in multiple pseudomonads (Fig. S1). Surprisingly, however, loss of *hopAS1b* has not yet been identified to significantly affect virulence of Psa3 V-13.

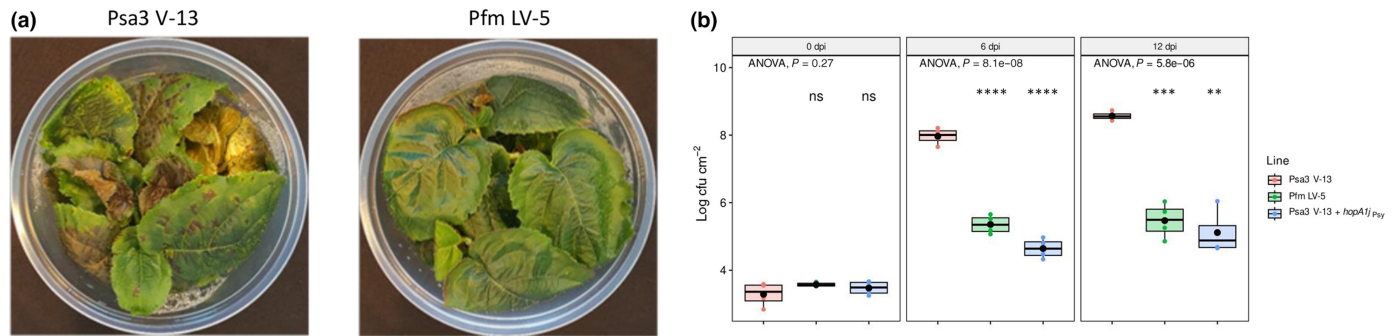


Fig. 1 *Pseudomonas syringae* pv. *actinidifoliorum* (Pfm) LV-5 lacks virulence in kiwifruit plants in comparison with *P. syringae* pv. *actinidiae* biovar 3 (Psa3) V-13. (a) *Actinidia chinensis* var. *chinensis* 'Hort16A' plantlets were flood inoculated with wild-type (WT) Psa3 V-13 or Pfm LV-5 at $c. 10^6$ CFU ml⁻¹. Photographs of symptom development on representative pottles of 'Hort16A' plantlets at 50 d postinfection. (b) 'Hort16A' plantlets were flood inoculated with WT Psa3 V-13, Pfm LV-5 or Psa3 V-13 carrying plasmid-borne avirulence effector *hopA1j* (from *P. syringae* pv. *syringae* 61) at $c. 10^6$ CFU ml⁻¹. Bacterial growth was quantified at 6- and 12 d postinoculation (dpi) by serial dilution and plate-count quantification. Box and whisker plots, with black bars representing the median values, black dots representing the means and whiskers representing the 1.5 \times interquartile range, for *in planta* bacterial counts plotted as log₁₀ CFU cm⁻² from four biological replicates. Asterisks indicate statistically significant differences from Welch's *t*-test between the indicated strain and WT Psa3 V-13: **, $P \leq 0.01$; ***, $P \leq 0.001$; ****, $P \leq 0.0001$; ns, not significant. These experiments were conducted three times on independent batches of 'Hort16A' plants, with similar results.

To investigate effector requirements and contribution to virulence in susceptible *A. chinensis* var. *chinensis* plants, a previously developed library of effector knockout strains was tested on 'Hort16A' plantlets and assessed for reduced *in planta* colonisation (Hemara *et al.*, 2022). Reductions in Psa3 V-13 growth, assessed at 6 and 12 dpi, were observed in Δ *hopS2b*, Δ *hopAZ1a* and Δ *xEEL* mutant strains (Figs 2a, S2). Despite having a similar topology to AvrE1d and HopR1b, loss of *hopAS1b* did not affect virulence of Psa3 V-13. Interestingly, unlike the symptom reduction seen previously for loss of effectors *avrE1d* (Δ *CEL*) and *hopR1b* (Jayaraman *et al.*, 2020), loss of these three effector loci was not associated with a reduction in disease symptom progression on the highly susceptible 'Hort16A' plants (Fig. 2b; Table S4). Plasmid complementation of effectors *hopS2b* (with its chaperone *shcS2*) and *hopAZ1a* in their respective knockout strains restored host colonisation (Fig. S3).

The ten-effector Δ *xEEL* knockout mutant resulted in a loss of virulence and contrasted with the eight-effector Δ *fEEL* knockout mutant that remained fully pathogenic (Figs 3a, S2). The additional two effectors lost (Δ *hopQ1a* and Δ *hopD1a*) in the Δ *xEEL* mutant were independently unable to affect virulence, suggesting redundancy between these two effectors or shared with effectors from the *fEEL* (Fig. S2). To investigate whether the additional two effectors lost (Δ *hopQ1a* and Δ *hopD1a*) were redundantly responsible for the contribution to virulence in the Δ *xEEL* mutant, a double knockout of these two effectors was generated and tested alongside Δ *fEEL* and Δ *xEEL* mutants (Fig. 3a). Notably, neither the Δ *fEEL* nor the Δ *hopQ1a/\Delta**hopD1a* mutant strains showed reduced virulence, suggesting that loss of effector redundancy or additive contributions from these effectors across the total set of 10 effectors in the *xEEL* locus was probably responsible for the change in the Δ *xEEL* mutant (Fig. 3b).

Screening all Psa3 V-13 effectors for PTI-suppression activity previously identified HopD1a as a potent contributor to PTI-suppression (Choi *et al.*, 2017). Interestingly, using *P. fluorescens* Pf0-1 (T3S) delivery for rescreening effectors from Psa3 V-13,

with a lower stringency (suppression was considered positive if at least two out of four infiltrated leaf patches showed a hypersensitive response), identified four Psa3 effectors that were able to suppress *P. fluorescens*-triggered PTI in *N. benthamiana* plants: HopD1a, AvrB2b, HopD2a and HopAW1a (Fig. S4). All four effectors lie within the *xEEL* locus and were able to suppress PTI to allow for the subsequent ETI triggered by Pto DC3000 to a capacity similar to but lower than that for the positive control, AvrPtoB from Pto DC3000 (Fig. S4). Testing of individual effector contributions to the Δ *xEEL* mutant by plasmid complementation confirmed that these four effectors were individually able to restore the Δ *xEEL* mutant's loss of virulence (Fig. 3c). To assess whether these effectors were also able to suppress PTI in their natural plant host, *A. chinensis* leaves were used to assess callose deposition (a PTI response) against *P. fluorescens* Pf0-1 (T3S) carrying empty vector or each of the four *xEEL* effectors (Fig. 3d). Notably, three out of the four effectors were able to significantly suppress callose deposition (Fig. 3d,e).

To determine whether the three effectors/loci (*hopS2*, *hopAZ1* and *xEEL*) additively contribute to virulence in 'Hort16A', cumulative knockouts were generated and tested for *in planta* colonisation and symptom development. These effector contributions were tested in the Δ *CEL* background where *avrE1d* contributes a large proportion of the virulence observed in Psa3 (Jayaraman *et al.*, 2020). Knockout of the *xEEL* in the Δ *CEL* background, or knockout of *hopS2b* and *hopAZ1a* in addition to Δ *CEL*, reduced virulence of the double and triple mutant strains, respectively, to a similar extent as that in the avirulent Δ *hrcC* mutant (Fig. 4a). Unsurprisingly, knocking out these effectors in addition to the loss of the *CEL* did not show disease progression differences from those seen in the symptomless Δ *CEL*-infected 'Hort16A' plants (Fig. 4b). Virulence was also tested for the quadruple-locus knockout of Δ *CEL/\Delta**xEEL/\Delta**hopS2b/\Delta**hopAZ1a* and found to be no different from the Δ *hrcC* mutant either (Fig. S5). Taken together, these assays have identified multiple effectors from three new loci (*hopAZ1a* and *hopS2b*, individually,

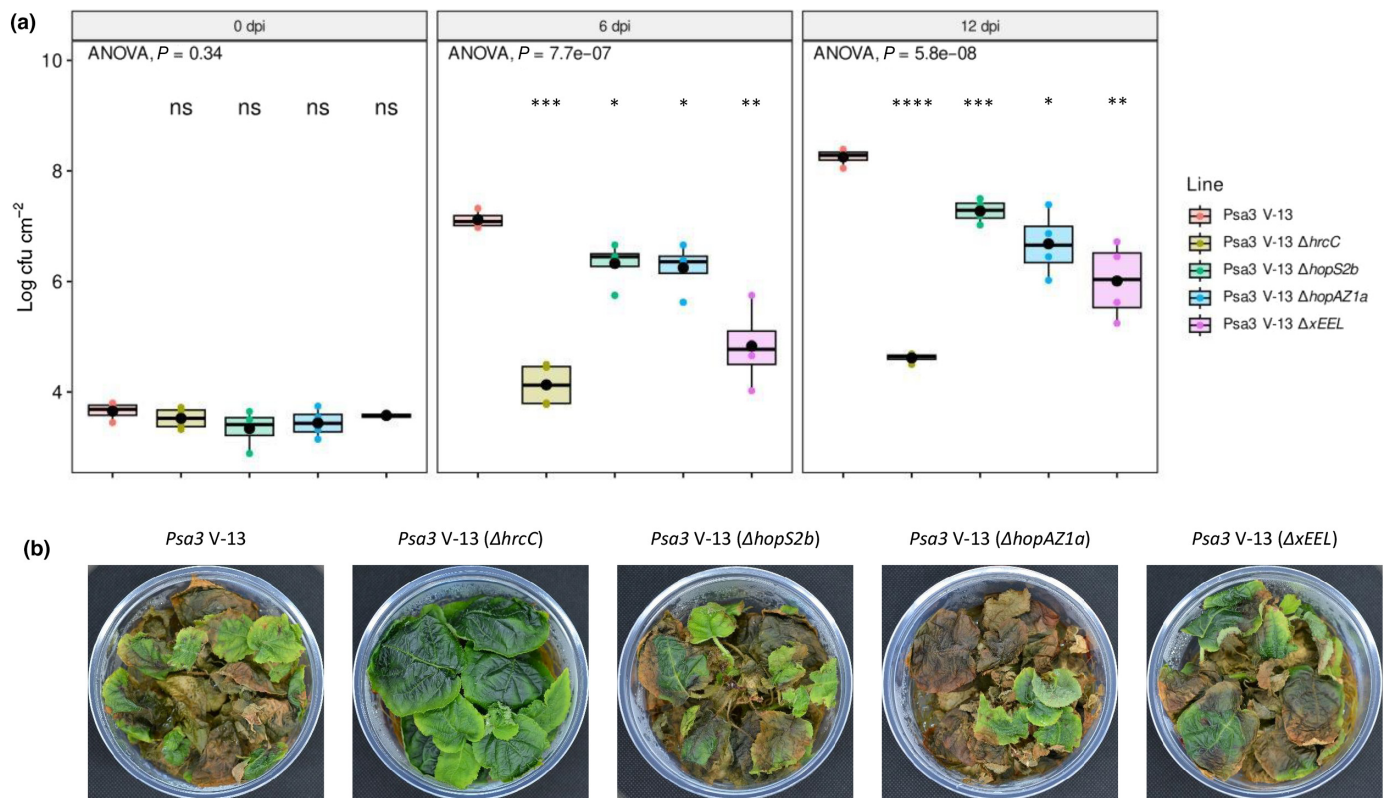


Fig. 2 Three *Pseudomonas syringae* pv. *actinidiae* biovar 3 (Psa3) V-13 effector loci are independently required for full virulence. *Actinidia chinensis* var. *chinensis* 'Hort16A' plantlets were flood inoculated with wild-type (WT) Psa3 V-13, $\Delta hrcC$ mutant, $\Delta hopS2b$ mutant, $\Delta hopAZ1a$ mutant or $\Delta xEEL$ (extended EEL) mutant at c. 10^6 CFU ml⁻¹. (a) Bacterial growth was quantified at 6- and 12 d postinoculation (dpi) by serial dilution and plate-count quantification. Box and whisker plots, with black bars representing the median values, black dots representing the means and whiskers representing the 1.5 \times interquartile range, for *in planta* bacterial counts plotted as log₁₀ CFU cm⁻² from four biological replicates. Asterisks indicate statistically significant differences from Welch's *t*-test between the indicated strain and WT Psa3 V-13: *, $P \leq 0.05$; **, $P \leq 0.01$; ***, $P \leq 0.001$; ****, $P \leq 0.0001$; ns, not significant. These experiments were conducted three times on independent batches of 'Hort16A' plants, with similar results. (b) Symptom development on representative pottles of 'Hort16A' plantlets infected with strains in (a) at 50 d postinfection.

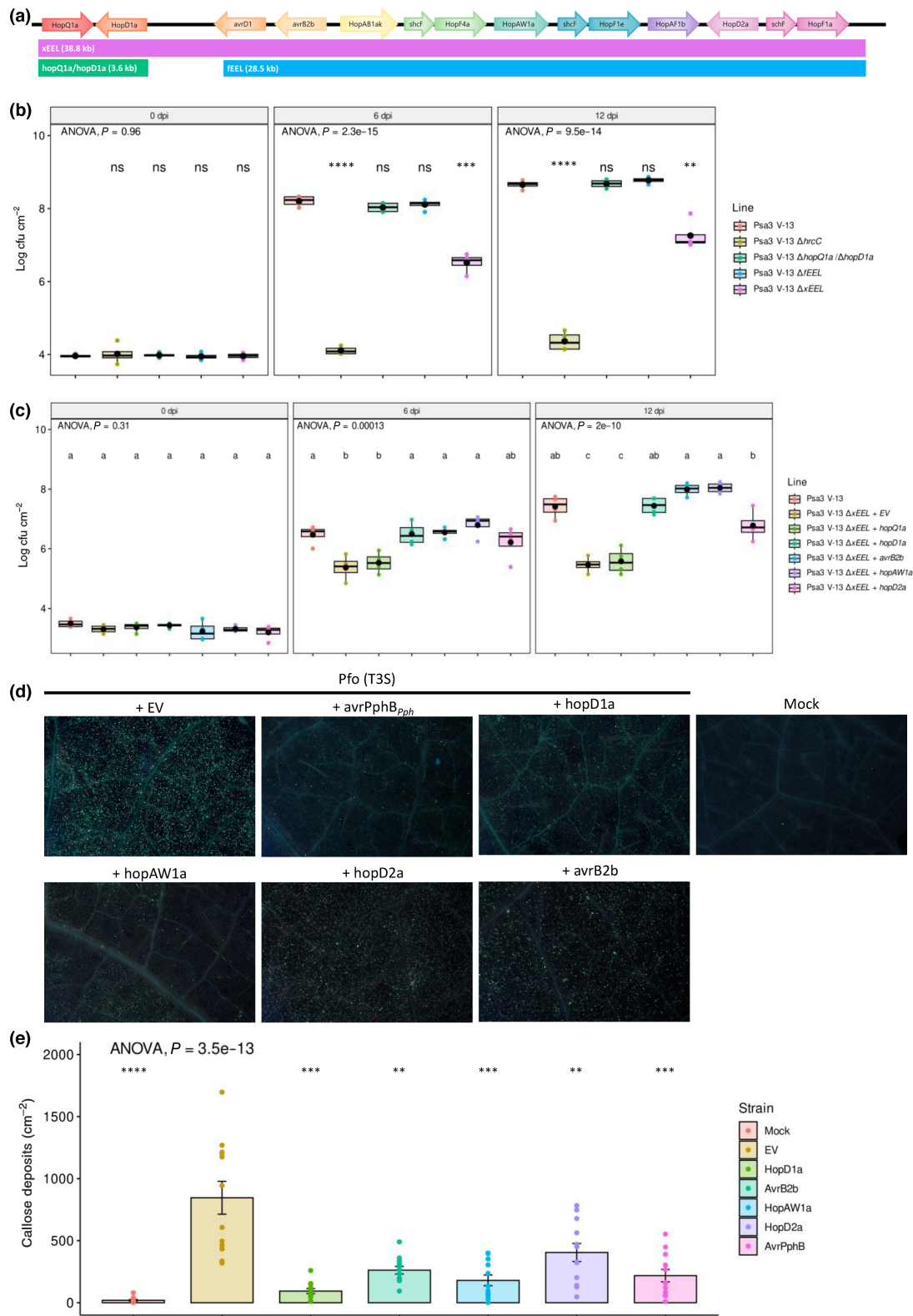
as well as a combination of *hopD1a*, *avrB2b*, *hopD2a* and *hopAW1a* from the *EEL* that nonredundantly and additively contribute to virulence of Psa3 in 'Hort16A' plants.

Avirulence effectors from Pfm cannot explain its lack of virulence in 'Hort16A'

The comparison of effector repertoires of Psa3 V-13 and Pfm LV-5 suggested only limited overlap with just 11 effectors shared

(Table S3). Surprisingly, four effectors (*avrE1d*, *hopR1b*, *hopS2b* and *hopAZ1a*) identified from Psa3 V-13 that individually contribute to virulence were also present in Pfm LV-5, along with required promoters and chaperones. The exception to required effectors in Psa3 also being present in Pfm were effectors from the *xEEL* in Psa3 V-13 (*hopD1a*, *avrB2b*, *hopD2a* and *hopAW1a*). Instead, effectors in Pfm LV-5, namely *hopW1f* and *hopA1a*, which are able to suppress PTI, probably substitute for these effectors (Fig. S6). A close ortholog of the positive control

Fig. 3 *Pseudomonas syringae* pv. *actinidiae* biovar 3 (Psa3) V-13 extended exchangeable effector locus (xEEL) carries four redundantly required PTI-suppressing effectors. (a) The extended EEL (xEEL) of Psa3 V-13 is made up of 10 effectors (*hopQ1a* to *hopF1a*) with a smaller subset of eight effectors (*avrD1* to *hopF1a*) designated as the full EEL (fEEL). (b) *Actinidia chinensis* var. *chinensis* 'Hort16A' plantlets were flood inoculated with wild-type (WT) Psa3 V-13, $\Delta hrcC$ mutant, $\Delta hopQ1a/\Delta hopD1a$ double mutant, $\Delta fEEL$ mutant or $\Delta xEEL$ mutant at c. 10^6 CFU ml⁻¹. Bacterial growth was quantified at 6- and 12 d postinoculation (dpi) by serial dilution and plate-count quantification. Asterisks indicate statistically significant differences from Welch's *t*-test between the indicated strain and WT Psa3 V-13, where **, $P \leq 0.01$; ***, $P \leq 0.001$ or ****, $P \leq 0.0001$; ns, not significant. (c) *A. chinensis* var. *chinensis* 'Hort16A' plantlets were flood inoculated with WT Psa3 V-13 carrying an empty vector (+EV), $\Delta xEEL$ mutant +EV or $\Delta xEEL$ mutant complemented with plasmid vector carrying *hopQ1a*, *hopD1a*, *avrB2b*, *hopAW1a* or *hopD2a* at c. 10^6 CFU ml⁻¹. Bacterial growth was quantified at 6- and 12 d postinoculation by serial dilution and plate-count quantification. In (b, c), data are presented as box and whisker plots, with black bars representing the median values, black dots representing the means and whiskers representing the 1.5 \times interquartile range, for *in planta* bacterial counts plotted as log₁₀ CFU cm⁻² from four biological replicates. Letters indicate statistically significant differences from a one-way ANOVA and Tukey's HSD *post hoc* test. These experiments were conducted three times on independent batches of 'Hort16A' plants, with similar results. (d) Callose deposition induced by *P. fluorescens* Pf0-1 (T3S) strain carrying empty vector (+EV), or positive control HopAR1 effector (+AvrPphB), or one of four Psa3 V-13 effectors from (b) in *A. chinensis* var. *deliciosa* leaves. The representative images were captured at 48 h after infiltration with mock (sterile 10 mM MgSO₄) or bacterial strains. (e) The number of callose deposits per cm² of leaf tissue from (d) was analysed with the IMAGEJ software. Mean and SE (SEM<) were calculated with results from five biological replicates. Different letters indicate significant difference from a one-way ANOVA and Tukey's HSD *post hoc* test at $P \leq 0.05$.



for the assay, AvrPtoB (HopAB1i from Pfm LV-5), may also be contributing to PTI-suppression but triggered an HR in *N. benthamiana*, and thus, its role could not be verified (Choi

et al., 2017). Additionally, testing of Psa3 V-13 effectors HopD1a, AvrB2b, HopD2a or HopAW1a failed to add to host colonisation ability of Pfm LV-5 (Fig. S7). These results

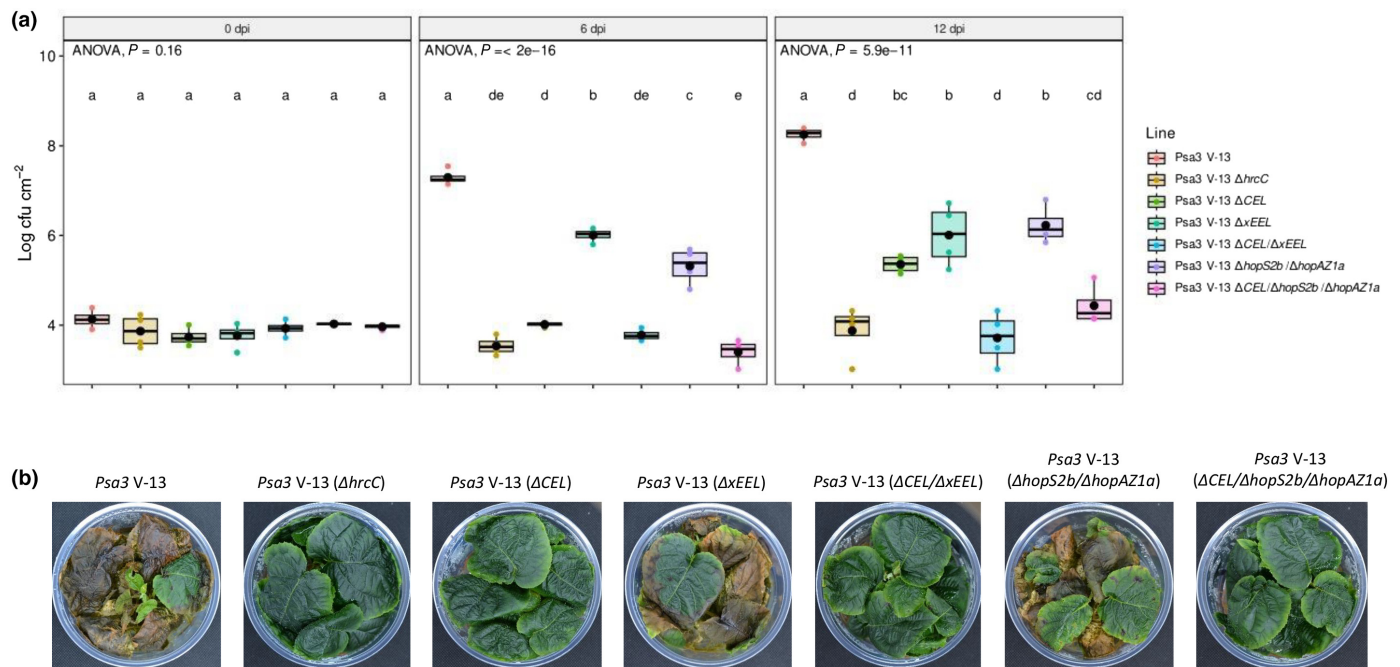


Fig. 4 *Pseudomonas syringae* pv. *actinidiae* biovar 3 (Psa3) V-13 virulence-associated effector loci are required alongside the conserved effector locus (CEL). *Actinidia chinensis* var. *chinensis* 'Hort16A' plantlets were flood inoculated with wild-type (WT) Psa3 V-13, $\Delta hrcC$ mutant, ΔCEL mutant, $\Delta xEEL$ mutant, $\Delta CEL/\Delta xEEL$ double mutant, $\Delta hopS2b/\Delta hopAZ1a$ double mutant or $\Delta CEL/\Delta hopS2b/\Delta hopAZ1a$ triple mutant at c. 10^6 CFU ml⁻¹. (a) Bacterial growth was quantified at 6- and 12 d postinoculation (dpi) by serial dilution and plate-count quantification. Box and whisker plots, with black bars representing the median values, black dots representing the means and whiskers representing the 1.5 \times interquartile range, for *in planta* bacterial counts plotted as log₁₀ CFU cm⁻² from four biological replicates. Letters indicate statistically significant differences from a one-way ANOVA and Tukey's HSD *post hoc* test. These experiments were conducted three times on independent batches of 'Hort16A' plants, with similar results. (b) Symptom development on representative pottles of 'Hort16A' plantlets infected with strains in (a) at 50 d postinfection.

suggested instead that there might be effectors carried by Pfm LV-5 that render it avirulent on 'Hort16A' plants.

Pfm LV-5 carries 16 effectors that are uniquely present when compared to Psa V-13 (absent in Psa3 V-13 or carrying an allele with < 90% identity to Psa3 V-13) with the potential to be avirulence effectors (Table S3). Each of these 16 effectors was cloned under a synthetic *avrRps4* promoter with a C-terminal HA tag, and most effectors were expressed when delivered by Psa3 V-13 (Fig. S8). Screening these Psa3 V-13 strains carrying Pfm LV-5 effectors on 'Hort16A' plants identified two effectors, *hopA1a* (10-fold reduction of virulence) and *hopE1a* (100-fold reduction in virulence) as candidate avirulence effectors (Fig. S9; Jayaraman *et al.*, 2017). Delivering HopE1a_{Pfm} also largely eliminated Psa3 V-13-induced disease symptoms in 'Hort16A', while HopA1a_{Pfm} delivery barely reduced virulence (Fig. S10). Since the C-terminal HA tag may possibly interfere with immunity triggered by an effector, each of these effectors was cloned under their native promoters, where possible, and delivered by Psa3 V-13. Again only HopA1a_{Pfm} and HopE1a_{Pfm} were associated with a reduction of Psa3 V-13 virulence in 'Hort16A' plants (Fig. S11). Using a reporter eclipse assay for candidate avirulence effectors as well as effectors poorly expressed *in vitro* also identified HopA1a_{Pfm} and HopE1a_{Pfm} as avirulence effectors in 'Hort16A' (Fig. S12).

Knockout of avirulence effectors should allow for increased growth of Pfm LV-5 in 'Hort16A'. Single and double-knockout

strains in Pfm LV-5 for $\Delta hopA1a$, $\Delta hopE1a$ or $\Delta hopA1a/\Delta hopE1a$ were generated and tested for *in planta* growth. Surprisingly, none of these effector knockouts showed increased virulence in 'Hort16A' plants compared with WT Pfm LV-5 or Psa3 V-13 (Fig. S13). Taken together, these findings suggest that Pfm LV-5 possesses all nonredundant virulence-associated effectors and its avirulence effectors do not contribute significantly to reduced virulence in 'Hort16A' plants.

Redundant virulence-associated effectors from Psa3 largely target host RIN4 proteins

In an attempt to understand the lack of virulence in Pfm LV-5 compared with Psa V-13, putatively redundant virulence-associated effectors were tested for their contribution to host colonisation. Since HopA1a and HopE1a may be contributing to low rates of growth restriction, the double-knockout strain Pfm LV-5 $\Delta hopA1a/\Delta hopE1a$ was used for plasmid complementation of Psa3 V-13-specific effectors (*avrB2b*, *avrPto1b*, *avrRpm1a*, *hopD1a*, *hopF1c*, *hopH1a*, *hopZ5a*, *hopI1c*, *hopM1f*, *hopQ1a*, *hopF4a*, *hopBP1a*, *hopAM1a*, *hopD2a*, *hopAU1a*, *hopAW1a*, *hopF1e* and *hopBN1a*). The expression of these HA-tagged Psa3 effectors in Pfm was validated under *hrp*-inducing conditions *in vitro* (Fig. S14). Five Psa3 effectors were found to quantitatively increase virulence of Pfm LV-5 $\Delta hopA1a/\Delta hopE1a$ on 'Hort16A' plants (Fig. 5a).

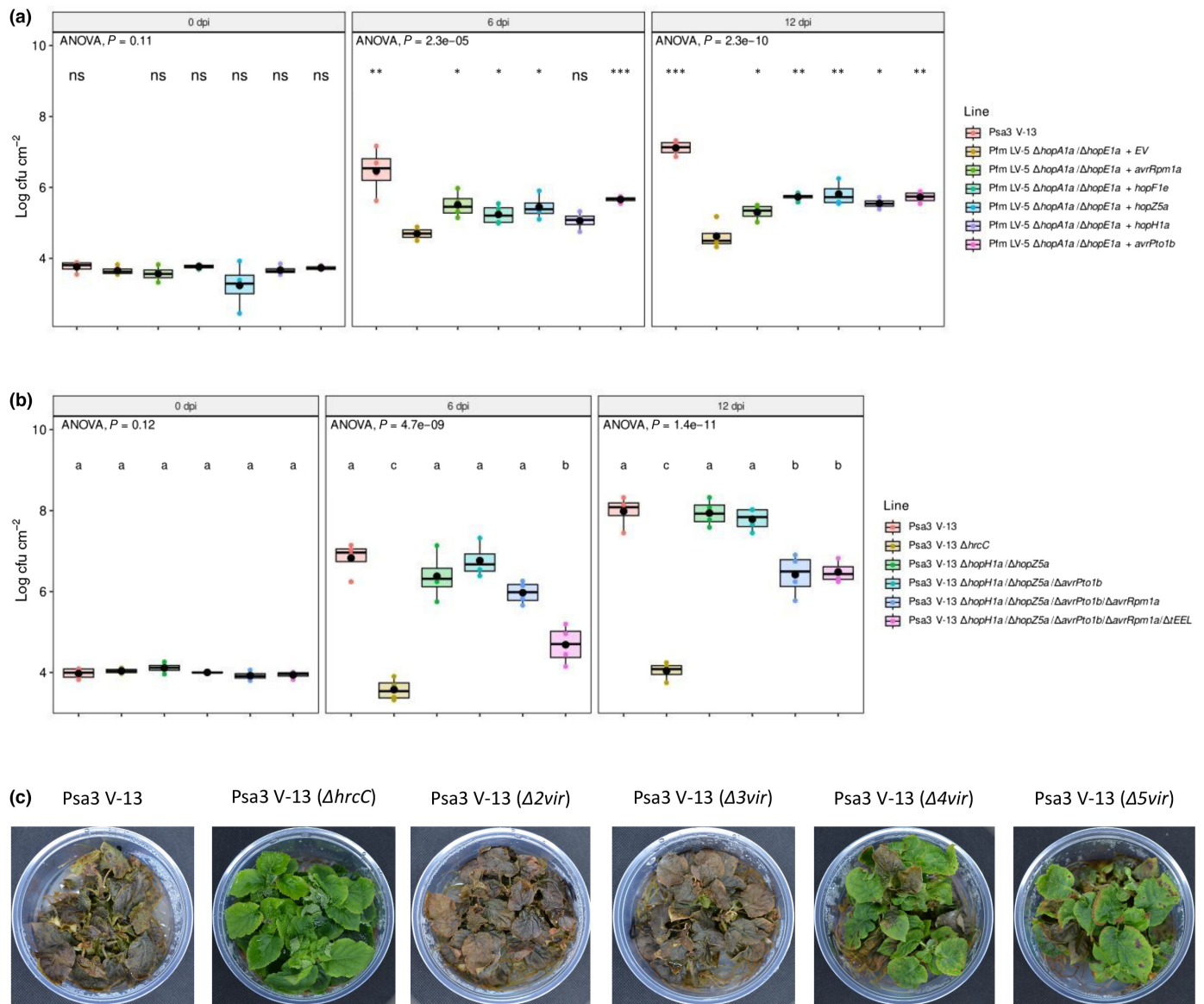


Fig. 5 Five *Pseudomonas syringae* pv. *actinidiae* biovar 3 (Psa3) V-13 effectors offer redundant contributions to virulence. (a) *Actinidia chinensis* var. *chinensis* 'Hort16A' plantlets were flood inoculated with wild-type (WT) Psa3 V-13, Pfm LV-5 $\Delta hopA1a/\Delta hopE1a$ double mutant or Pfm LV-5 $\Delta hopA1a/\Delta hopE1a$ double mutant complemented with plasmid-borne Psa3 V-13 effectors *avrRpm1a*, *hopF1e*, *hopZ5a*, *hopH1a* or *avrPto1b* at $c. 10^6$ CFU ml^{-1} . Bacterial growth was quantified at 6- and 12 d postinoculation (dpi) by serial dilution and plate-count quantification. Box and whisker plots, with black bars representing the median values and whiskers representing the $1.5\times$ interquartile range, for *in planta* bacterial counts plotted as \log_{10} CFU cm^{-2} from four biological replicates. Asterisks indicate statistically significant differences from Welch's *t*-test between the indicated strain and Pfm LV-5 $\Delta hopA1a/\Delta hopE1a$ double mutant: *, $P \leq 0.05$; **, $P \leq 0.01$; ***, $P \leq 0.001$; ns, not significant. These experiments were conducted three times on independent batches of 'Hort16A' plants, with similar results. (b) *Actinidia chinensis* var. *chinensis* 'Hort16A' plantlets were flood inoculated with WT Psa3 V-13, $\Delta hrcC$ mutant, $\Delta hopH1a/\Delta hopZ5a$ mutant, $\Delta hopH1a/\Delta hopZ5a/\Delta avrPto1b$ mutant, $\Delta hopH1a/\Delta hopZ5a/\Delta avrPto1b/\Delta avrRpm1a$ mutant or $\Delta hopH1a/\Delta hopZ5a/\Delta avrPto1b/\Delta avrRpm1a/\Delta tEEL$ mutant at $c. 10^6$ CFU ml^{-1} . Bacterial growth was quantified at 6- and 12 d postinoculation by serial dilution and plate-count quantification. Box and whisker plots, with black bars representing the median, black dots representing the means, values and whiskers representing the $1.5\times$ interquartile range, for *in planta* bacterial counts plotted as \log_{10} CFU cm^{-2} from four biological replicates. Letters indicate statistically significant differences from a one-way ANOVA and Tukey's HSD *post hoc* test. These experiments were conducted three times on independent batches of 'Hort16A' plants, with similar results. (c) Symptom development on representative pottles of 'Hort16A' plantlets infected with strains in (b) at 50 d postinfection.

The five virulence-associated Psa3 effectors (*hopZ5a*, *hopH1a*, *avrPto1b*, *avrRpm1a* and *hopF1e*) that contribute to Pfm LV-5 *in planta* growth did not alter virulence when knocked out individually in Psa3 V-13, suggesting that some redundancy across these effectors exists (Fig. S15). To confirm this, cumulative knockouts

of these effectors in Psa3 V-13 were generated and tested on 'Hort16A' plants. Notably, the Psa3 quadruple ($\Delta hopH1a/\Delta hopZ5a/\Delta avrPto1b/\Delta avrRpm1a$) and quintuple ($\Delta hopH1a/\Delta hopZ5a/\Delta avrPto1b/\Delta avrRpm1a/\Delta tEEL$) knockouts showed a large drop in virulence, confirming a redundant contribution of

at least some of these effectors to virulence (Fig. 5b). The quadruple and quintuple mutants were also considerably reduced in symptom development (Fig. 5c).

Three out of these five putatively redundant effectors in Psa3, or their orthologs in other plant–pathogen systems, have recently been shown to target the plant immunity hub RIN4 (Yoon & Rikkerink, 2020; Choi *et al.*, 2021; Jeleńska *et al.*, 2021). HopF1e and HopH1 have not been characterised for their *in planta* targets, but HopF1e is part of the larger HopF family that has members known to interact with RIN4 (Lo *et al.*, 2017). Indeed, Psa strains carry a large number of putative RIN4-targeting effectors (Hemara *et al.*, 2022). These predicted Psa3 RIN4-targeting effectors, including HopF family effectors or Psa orthologs of known RIN4-targeting effectors that were not associated with increased Pfm LV-5 $\Delta hopA1a/\Delta hopE1a$ growth, were tested for binding to RIN4 alleles from ‘Hort16A’. Co-immunoprecipitation screens were conducted in *N. benthamiana* plants with co-expression of alleles from one of three AcRIN4 loci and the effector of interest, as done previously for AvrRpm1a (Yoon & Rikkerink, 2020). The virulence-associated effectors (HopZ5a, HopH1a, AvrPto1b and HopF1e), known orthologs of RIN4 targeting effectors (HopBP1a and HopF1c) or putative HopF family effectors (HopF4a and HopBN1a) tested were all YFP-tagged and used to pull down any interacting FLAG-tagged RIN4 alleles (Fig. 6). Notably, three out of the four redundant virulence-associated effectors (HopZ5a, HopF1e and AvrPto1b) pulled down at least two alleles of AcRIN4. No interaction was seen for HopH1a, similar to the negative control YFP alone. Meanwhile, both HopF1c and HopF4a also pulled down AcRIN4 alleles, but are not associated with increases in virulence in Pfm LV-5, while HopBP1a and HopBN1a did not pull down AcRIN4 alleles. These results collectively suggest that AcRIN4 is a key target for a large number of Psa3 effectors that act together in a dynamic complex to facilitate ‘Hort16A’ infection.

Discussion

This work sought to identify the virulence determinants that make Psa3 strains hypervirulent on the susceptible kiwifruit cultivar ‘Hort16A’, particularly in contrast to the various other *Pseudomonas* species that occupy the kiwifruit phyllosphere. Using a commensal, low virulence kiwifruit-colonising Pfm strain to search for virulence amplifiers in a double effector knockout strain (Pfm LV-5 $\Delta hopA1a/\Delta hopE1a$), several redundantly acting effectors that largely target RIN4 were identified. While these effectors are collectively essential for full Psa3 virulence, no effectors were able to confer strong virulence to Pfm by themselves. This is despite Pfm being capable of causing disease on both sour cherry and pepper fruits (Ferrante & Scortichini, 2015). This underscores the complexity of virulence in plant-colonising bacterial strains and suggests that factors beyond their effector repertoires may contribute to virulence.

For the well-characterised tomato and Arabidopsis pathogen Pto DC3000 in its infection of nonhost *Nicotiana benthamiana* (or its native host tomato), several effectors were found to contribute towards virulence following the loss of avirulence effector

HopQ1 (Kvitko *et al.*, 2009; Cunnac *et al.*, 2011; Wei *et al.*, 2018). The AvrE1/HopM1/HopR1 redundant effector group (REG) was found to contribute to an aqueous apoplast, and the AvrPto/AvrPtoB REG was found to target and suppress PTI (Kvitko *et al.*, 2009). HopE1 supported increased growth *in planta*; HopG1 and HopAM1 were found to promote chlorotic and/or necrotic symptomology; and HopAA1 functioned redundantly with the phytotoxin coronatine to promote symptoms (Munkvold *et al.*, 2009; Cunnac *et al.*, 2011; Rodríguez-Puerto *et al.*, 2022). The vast majority of Pto DC3000 effectors appear to have an ETI-suppression role (Jamir *et al.*, 2004; Guo *et al.*, 2009). By contrast, Psa3 appears to have few REG members in common with Pto DC3000. Notably, the contributions of AvrE1d and HopR1b that form a REG in Pto DC3000 have nonredundant roles in virulence on kiwifruit hosts (Jayaraman *et al.*, 2020). In addition, this putative structure is also seen in HopAS1b, which forms a similar potentially ‘pore-forming’ structure to AvrE1d/HopR1b, but appears not to be required for virulence in kiwifruit plants (Figs S1, S2). Notably, these three effectors were the only cell death-triggering Psa3 effectors that did not show a reduction in cell death upon silencing of *SGT1* in *N. benthamiana*, suggesting that all three are functional and that their virulence function may be associated with triggering cell death (Choi *et al.*, 2017). Nevertheless, the variation among these three effectors’ requirements in Psa3 infection of kiwifruit plants suggests that the link between structural similarity and function is complex.

This work has identified two individual effectors (HopAZ1a and HopS2b) that contribute to host colonisation but have no effect on disease symptoms. This may be a unique role of these effectors that are not involved in symptom production, or a quantitative contribution that, despite affecting *in planta* accumulation, still allows for Psa3 colonisation beyond a threshold which then allows for symptom development (Stroud *et al.*, 2022). Collectively, these nonredundant effectors or effector ‘sets’ additively are essential for full virulence in ‘Hort16A’ plants. Recently, HopAZ1a from Psa3 has been associated with targeting defence-associated PR5 and a cysteine peptidase Cp1 in kiwifruit plants (Zhu *et al.*, 2022). This aforementioned work showed increased virulence for the $\Delta hopAZ1a$ mutant, unlike the reduced growth seen for our results. However, their use of different cultivars of kiwifruit, and use of quantitative symptom development alone, may explain this discrepancy. Nevertheless, the finding that HopAZ1a targets secreted protein PR5 (and possibly Cp1) fits with previous work that showed HopAZ1a localised to what appears to be endoplasmic reticulum-like structures, suggesting that it may target defence-related secretion (Choi *et al.*, 2017). While the plant targets of HopS2b are not known, a close ortholog of this effector from Pto DC3000 is a strong suppressor of ETI (Guo *et al.*, 2009). Recently, the HopS family of ADP-ribosyl transferases were identified as significant contributors to virulence and ETI-suppression through activity as NADases (Hulin *et al.*, 2023). HopAZ1a and HopS2b appear to be the only effectors present universally across the five Psa biovars and Pfm, suggesting they play an important role in kiwifruit plant colonisation (McCann *et al.*, 2013; Sawada & Fujikawa, 2019).

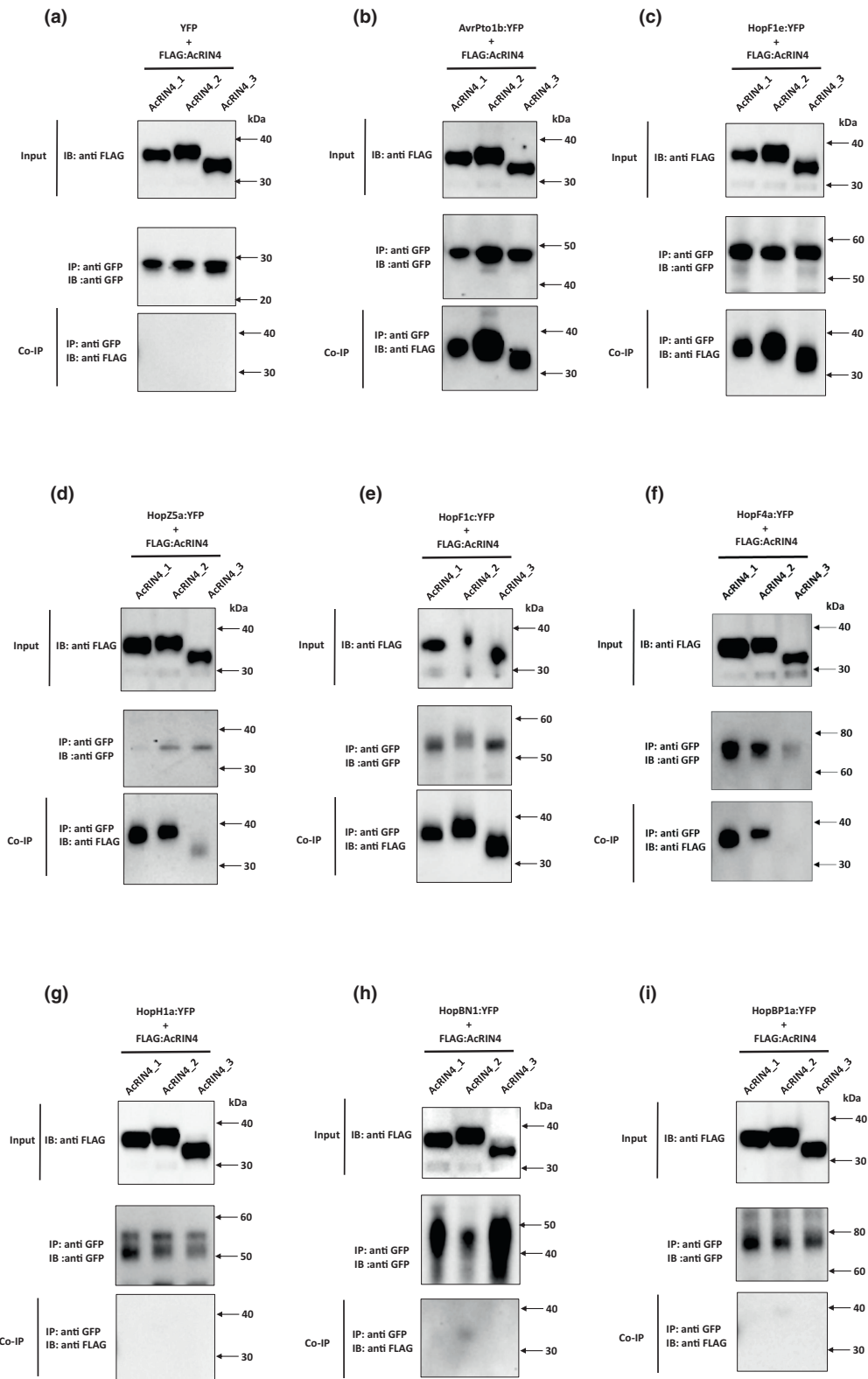


Fig. 6 *Pseudomonas syringae* pv. *actinidiae* biovar 3 (Psa3) V-13 redundant virulence-associated effectors largely target kiwifruit RIN4 proteins. Co-immunoprecipitation of YFP (a), or effectors AvrPto1b (b), HopF1e (c), HopZ5a (d), HopF1c (e), HopF4a (f), HopH1a (g), HopBN1a (h), or HopBP1a (i) and target RIN4 proteins (AcRIN4-1, -2, or -3). YFP-tagged effectors (or YFP alone) and FLAG-tagged RIN4 homologs were expressed simultaneously by *Agrobacterium tumefaciens*-mediated transient expression under a CaMV 35S promoter. Two days after infiltration, leaf samples from a single plant were harvested, and protein extracts prepared and precipitated using anti-green fluorescent protein (GFP) antibody. A western blot from precipitated proteins was probed with anti-GFP (top) or anti-FLAG antibody (bottom). The plants were infiltrated with *Agrobacterium* at individual OD₆₀₀ of 0.1. IP, immunoprecipitation; IB, immunoblotting.

Using the same ‘single knockout’ approach used to identify the four nonredundant effectors contributing to virulence of Psa3 on ‘Hort16A’, the exchangeable effector locus (EEL) was also identified as a significant contributor to virulence. Interestingly, the entire extended EEL (xEEL) spanning 10 effectors from *hopQ1a* to *hopF1a* was redundantly required for this contribution to virulence. By using effector complementation, the xEEL was found to carry several functionally redundant effectors that participate in PTI-suppression: HopD1a, AvrB2b, HopAW1a and HopD2a. These effectors appear to be able to facilitate PTI-suppression in the same way that AvrPto/AvrPtoB redundantly contribute to PTI-suppression for Pto DC3000, and AvrPphB does for *P. syringae* pv. *phaseolicola* (Hann & Rathjen, 2007; Kvitko *et al.*, 2009; Zhang *et al.*, 2010).

Several redundant Psa3 effectors were identified that could contribute to Pfm virulence when expressed in *trans*: HopZ5a, AvrRpm1a, HopF1e, AvrPto5 and HopH1a. AvrRpm1a has been shown previously to target AcrIN4 alleles (Yoon & Rikkerink, 2020). In our current work, three out of the other four of these redundant virulence-associated effectors were shown to directly interact with AcrIN4 orthologs, suggesting a mechanism of virulence conserved in Psa3. This latter screen also tested all Psa3 effectors that are part of the HopF family (HopBN1a, HopF4a, HopF1c and HopF1e), which has members known to target RIN4 as well as other orthologs that have been shown to target RIN4 (Wilton *et al.*, 2010; Lo *et al.*, 2017; Choi *et al.*, 2021; Jeleńska *et al.*, 2021). Several of these effectors showed interesting relationships between their ability to target AcrIN4 and their contribution to virulence. HopH1a was the sole effector associated with virulence that did not bind to AcrIN4, while effectors HopF1c and HopF4a surprisingly did bind AcrIN4 but were not associated with virulence (Fig. 6). One reason that HopF1c was not identified is that it carries a defective SchF chaperone (Templeton *et al.*, 2015). HopF1c has also previously been associated with triggering ETI in ‘Hort16A’ but is probably suppressed by other Psa3 effectors, so it is not surprising that it does not contribute to Pfm virulence (Hemara *et al.*, 2022). Meanwhile, the genomic sequence of *hopF4a* and its associated upstream *shcF* gene carries a transposon insertion that has deleted the SchF N terminus and separates *hopF4a* from its *hrpL* promoter (Templeton *et al.*, 2015). This predicted disruption is corroborated by RNA-seq data showing HopF4a (previously named HopX3) does not appear to be expressed *in planta* (McAtee *et al.*, 2018). HopF4a further lacks a functional catalytic triad from peptide sequence alignments and appears to be an enzymatically nonfunctional member of the HopF family (Fig. S16). HopBP1a (an ortholog of HopZ3 from *P. syringae* pv. *syringae* B728A that binds RIN4) did not bind to AcrIN4 and could not be confirmed as contributing to Pfm virulence, due to undetectable expression when delivered by Pfm (Fig. S14). Pfm LV-5 may require the AcrIN4-targeting capabilities supplied by these various effectors from Psa3 V-13 to increase Pfm virulence in kiwifruit plants.

The ability of the RIN4-targeting set of effectors to increase Pfm virulence implies they are also likely to be carrying out a similar role in Psa3. Why were these effectors not individually

identified as contributing to virulence in our screens? *A. arguta* plant lines like AA07_03 have evolved to recognise at least three of these effectors, and their deletion leads to an increase in fitness (Hemara *et al.*, 2022). This illustrates the active role being played by these RIN4-interacting effectors in the evolution of Psa and kiwifruit germplasm near the likely point of origin of Psa as a species (McCann *et al.*, 2017). In our analysis focussed on ‘Hort16A’, we suggest this is probably because of a complex series of interactions and active selection operating in both the host and pathogen around this important plant defence hub that is targeted by several different effector families across multiple bacterial plant pathogens (Sun *et al.*, 2014; Rikkerink, 2018; Toruño *et al.*, 2019). For example, in the case of the Psa3-susceptible ‘Hort16A’ host recognising hopF1c, the presence of this resistance (if now widespread in the wild kiwifruit-containing forests where Psa evolved) could well have resulted in selection for mutation of the associated chaperone SchF to reduce effector delivery. Finally, evidence in this work and previously suggests that there is a degree of redundancy among these effectors, as a cumulative loss of virulence on ‘Hort16A’ was evident in strains with multiple mutations in some RIN4-interacting effectors and HopH1a (Fig. 5; Hemara *et al.*, 2022). Applying the principle of Occam’s razor would suggest their association with RIN4 is probably responsible for this redundancy.

A corollary question then becomes – what is the importance of targeting RIN4? Three effectors associated with RIN4 that trigger HR in *A. arguta* unusually did not trigger the ion leakage usually associated with this response (Hemara *et al.*, 2022). This may indicate that one reason for targeting RIN4 is associated with suppressing ion leakage, a physiological response that is largely due to the loss of membrane integrity and is associated with the programmed cell death component of the HR. Thus, it is conceivable that RIN4 performs an important regulatory function in controlling the initiation of (or limitation of) HR-associated cell death. The role of RIN4 in at least some hybrid-necrosis responses in lettuce could be an important functional clue here, albeit also probably in association with NLR proteins (Jeuken *et al.*, 2009; Parra *et al.*, 2016). The disordered protein structure of RIN4 has been suggested to be a key component that explains how it has evolved into such an important defence hub and target of post-translational modification by bacterial pathogens (Sun *et al.*, 2014; Rikkerink, 2018). When our recent results are combined with previous research, it is increasingly clear that RIN4 is an equally important target for Psa (Yoon & Rikkerink, 2020).

Acknowledgements

This work was funded by the Bio-protection Research Centre (Tertiary Education Commission) and the Royal Society Te Apārangi (including a Marsden FastStart grant and Rutherford Foundation postdoctoral fellowship to JJ). LMH is funded by a University of Auckland PhD scholarship. We would like to thank Dr Jo Bowen (PFR) and Prof. Andrew Allan (PFR) for critical reading of this manuscript. The authors wish to acknowledge the use of New Zealand eScience Infrastructure (NeSI) high-performance computing facilities as part of this research. New

Zealand's national facilities are provided by NeSI and funded jointly by NeSI's collaborator institutions and through the Ministry of Business, Innovation & Employment's Research Infrastructure programme. URL <https://www.nesi.org.nz>. Open access publishing facilitated by New Zealand Institute for Plant and Food Research Ltd, as part of the Wiley - New Zealand Institute for Plant and Food Research Ltd agreement via the Council of Australian University Librarians.





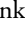



Competing interests

None declared.

Author contributions

JJ, CB, EHAR and MDT planned and designed the research. JJ, MY, LMH, DB, JT and RKYC performed experiments, analysed data and prepared figures. JJ, EHAR and MDT wrote the manuscript.

ORCID

Cyril Brendolise  <https://orcid.org/0000-0001-8213-8094>
 Ronan K. Y. Chen  <https://orcid.org/0000-0002-2471-4628>
 Lauren M. Hemara  <https://orcid.org/0000-0003-0316-3545>
 Jay Jayaraman  <https://orcid.org/0000-0003-4959-9467>
 Erik H. A. Rikkerink  <https://orcid.org/0000-0003-4682-5078>
 Jibrán Tahir  <https://orcid.org/0000-0001-5134-6245>
 Matthew D. Templeton  <https://orcid.org/0000-0003-0192-9041>
 Minsoo Yoon  <https://orcid.org/0000-0001-5524-3972>

Data availability

The data that support the findings of this study are available on request from the corresponding author. The data are not publicly available due to privacy or ethical restrictions.

References

- Abelleira A, Ares A, Aguin O, Peñalver J, Morente MC, López MM, Sainz MJ, Mansilla JP. 2015. Detection and characterization of *Pseudomonas syringae* pv. *actinidifoliorum* in kiwifruit in Spain. *Journal of Applied Microbiology* 119: 1659–1671.
- Bartoli C, Lamichhane JR, Berge O, Guilbaud C, Varvaro L, Balestra GM, Vinatzer BA, Morris CE. 2015. A framework to gauge the epidemic potential of plant pathogens in environmental reservoirs: the example of kiwifruit canker: the epidemic potential of plant pathogens. *Molecular Plant Pathology* 16: 137–149.
- Boller T, Felix G. 2009. A renaissance of elicitors: perception of microbe-associated molecular patterns and danger signals by pattern-recognition receptors. *Annual Review of Plant Biology* 60: 379–406.
- Chapman JR, Taylor RK, Weir BS, Romberg MK, Vanneste JL, Luck J, Alexander BJR. 2012. Phylogenetic relationships among global populations of *Pseudomonas syringae* pv. *actinidiae*. *Phytopathology* 102: 1034–1044.
- Chen T, Nomura K, Wang X, Sohrabi R, Xu J, Yao L, Paasch BC, Ma L, Kremer J, Cheng Y *et al.* 2020. A plant genetic network for preventing dysbiosis in the phyllosphere. *Nature* 580: 653–657.
- Choi S, Jayaraman J, Segonzac C, Park H-J, Park H, Han S-W, Sohn KH. 2017. *Pseudomonas syringae* pv. *actinidiae* type III effectors localized at multiple cellular compartments activate or suppress innate immune responses in *Nicotiana benthamiana*. *Frontiers in Plant Science* 8: 2157.
- Choi S, Prokhorchik M, Lee H, Gupta R, Lee Y, Chung E-H, Cho B, Kim M-S, Kim ST, Sohn KH. 2021. Direct acetylation of a conserved threonine of RIN4 by the bacterial effector HopZ5 or AvrBsT activates RPM1-dependent immunity in Arabidopsis. *Molecular Plant* 14: 1951–1960.
- Crabill E, Joe A, Block A, van Rooyen JM, Alfano JR. 2010. Plant immunity directly or indirectly restricts the injection of type III effectors by the *Pseudomonas syringae* type III secretion system. *Plant Physiology* 154: 233–244.
- Cunnac S, Chakravarthy S, Kvitko BH, Russell AB, Martin GB, Collmer A. 2011. Genetic disassembly and combinatorial reassembly identify a minimal functional repertoire of type III effectors in *Pseudomonas syringae*. *Proceedings of the National Academy of Sciences, USA* 108: 2975–2980.
- Cunty A, Poliakoff F, Rivoal C, Cesbron S, Fischer-Le Saux M, Lemaire C, Jacques MA, Manceau C, Vanneste JL. 2015. Characterization of *Pseudomonas syringae* pv. *actinidiae* (Psa) isolated from France and assignment of Psa biovar 4 to a *de novo* pathovar: *Pseudomonas syringae* pv. *actinidifoliorum* pv. nov. *Plant Pathology* 64: 582–596.
- DeFalco TA, Zipfel C. 2021. Molecular mechanisms of early plant pattern-triggered immune signaling. *Molecular Cell* 81: 3449–3467.
- Diallo MD, Monteil CL, Vinatzer BA, Clarke CR, Glaux C, Guilbaud C, Desbiez C, Morris CE. 2012. *Pseudomonas syringae* naturally lacking the canonical type III secretion system are ubiquitous in nonagricultural habitats, are phylogenetically diverse and can be pathogenic. *The ISME Journal* 6: 1325–1335.
- Ferrante P, Scortichini M. 2015. Redefining the global populations of *Pseudomonas syringae* pv. *actinidiae* based on pathogenic, molecular and phenotypic characteristics. *Plant Pathology* 64: 51–62.
- Gentzel I, Giese L, Ekanayake G, Mikhail K, Zhao W, Cocuron J-C, Alonso AP, Mackey D. 2022. Dynamic nutrient acquisition from a hydrated apoplast supports biotrophic proliferation of a bacterial pathogen of maize. *Cell Host & Microbe* 30: 502–517.
- Guo M, Tian F, Wamboldt Y, Alfano JR. 2009. The majority of the type III effector inventory of *Pseudomonas syringae* pv. *tomato* DC3000 can suppress plant immunity. *Molecular Plant–Microbe Interactions* 22: 1069–1080.
- Hann DR, Rathjen JP. 2007. Early events in the pathogenicity of *Pseudomonas syringae* on *Nicotiana benthamiana*. *The Plant Journal* 49: 607–618.
- Hemara LM, Jayaraman J, Sutherland PW, Montefiori M, Arshed S, Chatterjee A, Chen R, Andersen MT, Mesarich CH, van der Linden O *et al.* 2022. Effector loss drives adaptation of *Pseudomonas syringae* pv. *actinidiae* biovar 3 to *Actinidia arguta*. *PLoS Pathogens* 18: e1010542.
- Hulin MT, Hill L, Jones JDG, Ma W. 2023. Pangenomic analysis reveals plant NAD⁺ manipulation as an important virulence activity of bacterial pathogen effectors. *Proceedings of the National Academy of Sciences, USA* 120: e2217114120.
- Hunter DA, Watson LM. 2008. The harvest-responsive region of the *Asparagus officinalis* sparagine synthetase promoter reveals complexity in the regulation of the harvest response. *Functional Plant Biology* 35: 1212–1223.
- Huynh T, Dahlbeck D, Staskawicz B. 1989. Bacterial blight of soybean: regulation of a pathogen gene determining host cultivar specificity. *Science* 245: 1374–1377.
- Jamir Y, Guo M, Oh H-S, Petnicki-Ocwieja T, Chen S, Tang X, Dickman MB, Collmer A, Alfano JR. 2004. Identification of *Pseudomonas syringae* type III effectors that can suppress programmed cell death in plants and yeast. *The Plant Journal* 37: 554–565.
- Jayaraman J, Chatterjee A, Hunter S, Chen R, Stroud EA, Saei H, Hoyte S, Deroles S, Tahir J, Templeton MD *et al.* 2021. Rapid methodologies for assessing *Pseudomonas syringae* pv. *actinidiae* colonization and effector-mediated hypersensitive response in kiwifruit. *Molecular Plant–Microbe Interactions* 34: 880–890.
- Jayaraman J, Choi S, Prokhorchik M, Choi DS, Spiandore A, Rikkerink EH, Templeton MD, Segonzac C, Sohn KH. 2017. A bacterial acetyltransferase triggers immunity in *Arabidopsis thaliana* independent of hypersensitive response. *Scientific Reports* 7: 3557.

- Jayaraman J, Yoon M, Applegate ER, Stroud EA, Templeton MD. 2020. AvrE1 and HopR1 from *Pseudomonas syringae* pv. *actinidiae* are additively required for full virulence on kiwifruit. *Molecular Plant Pathology* 21: 1467–1480.
- Jelenska J, Lee J, Manning AJ, Wolfgeher DJ, Ahn Y, Walters-Marras G, Lopez IE, Garcia L, McClerkin SA, Michelmore RW *et al.* 2021. *Pseudomonas syringae* effector HopZ3 suppresses the bacterial AvrPto1–tomato PTO immune complex via acetylation. *PLoS Pathogens* 17: e1010017.
- Jeuken MJW, Zhang NW, McHale LK, Pelgrom K, den Boer E, Lindhout P, Michelmore RW, Visser RGF, Niks RE. 2009. *Rin4* causes hybrid necrosis and race-specific resistance in an interspecific lettuce hybrid. *Plant Cell* 21: 3368–3378.
- Jin L, Mackey DM. 2017. Measuring callose deposition, an indicator of cell wall reinforcement, during bacterial infection in Arabidopsis. In: Shan L, He P, eds. *Plant pattern recognition receptors: methods in molecular biology*. New York, NY, USA: Springer, 195–205.
- Jumper J, Evans R, Pritzel A, Green T, Figurnov M, Ronneberger O, Tunyasuvunakool K, Bates R, Židek A, Potapenko A *et al.* 2021. Highly accurate protein structure prediction with AlphaFold. *Nature* 596: 583–589.
- Kovach ME, Elzer PH, Steven Hill D, Robertson GT, Farris MA, Roop RM, Peterson KM. 1995. Four new derivatives of the broad-host-range cloning vector pBBR1MCS, carrying different antibiotic-resistance cassettes. *Gene* 166: 175–176.
- Kvitko BH, Park DH, Velásquez AC, Wei C-F, Russell AB, Martin GB, Schneider DJ, Collmer A. 2009. Deletions in the repertoire of *Pseudomonas syringae* pv. *tomato* DC3000 type III secretion effector genes reveal functional overlap among effectors. *PLoS Pathogens* 5: e1000388.
- Laemmli UK. 1970. Cleavage of structural proteins during the assembly of the head of bacteriophage T4. *Nature* 227: 680–685.
- Le Roux C, Huet G, Jauneau A, Camborde L, Trémousaygue D, Kraut A, Zhou B, Levaillant M, Adachi H, Yoshioka H *et al.* 2015. A receptor pair with an integrated decoy converts pathogen disabling of transcription factors to immunity. *Cell* 161: 1074–1088.
- Levy A, Salas Gonzalez I, Mittelviefhaus M, Clingenpeel S, Herrera Paredes S, Miao J, Wang K, Devescovi G, Stillman K, Monteiro F *et al.* 2018. Genomic features of bacterial adaptation to plants. *Nature Genetics* 50: 138–150.
- Lo T, Koulouli N, Seto D, Guttman DS, Desveaux D. 2017. The HopF family of *Pseudomonas syringae* type III secreted effectors: the HopF family of *Pseudomonas syringae*. *Molecular Plant Pathology* 18: 457–468.
- Luna E, Pastor V, Robert J, Flors V, Mauch-Mani B, Ton J. 2011. Callose deposition: a multifaceted plant defense response. *Molecular Plant–Microbe Interactions* 24: 183–193.
- Mackey D, Belkhadir Y, Alonso JM, Ecker JR, Dangl JL. 2003. Arabidopsis RIN4 is a target of the type III virulence effector AvrRpt2 and modulates RPS2-mediated resistance. *Cell* 112: 379–389.
- Mackey D, Holt BF, Wiig A, Dangl JL. 2002. RIN4 interacts with *Pseudomonas syringae* type III effector molecules and is required for RPM1-mediated resistance in Arabidopsis. *Cell* 108: 743–754.
- Mazo-Molina C, Mainiero S, Hind SR, Kraus CM, Vachev M, Maviane-Macia F, Lindeberg M, Saha S, Strickler SR, Feder A *et al.* 2019. The *Prr1* locus of *Solanum lycopersicoides* confers resistance to Race 1 strains of *Pseudomonas syringae* pv. *tomato* and to *Ralstonia pseudosolanacearum* by recognizing the type III effectors AvrRpt2 and RipBN. *Molecular Plant–Microbe Interactions* 32: 949–960.
- McAtee PA, Brian L, Curran B, van der Linden O, Nieuwenhuizen NJ, Chen X, Henry-Kirk RA, Stroud EA, Nardoza S, Jayaraman J *et al.* 2018. Re-programming of *Pseudomonas syringae* pv. *actinidiae* gene expression during early stages of infection of kiwifruit. *BMC Genomics* 19: 822.
- McCann HC, Li L, Liu Y, Li D, Pan H, Zhong C, Rikkerink EHA, Templeton MD, Straub C, Colombi E *et al.* 2017. Origin and evolution of the kiwifruit canker pandemic. *Genome Biology and Evolution* 9: 932–944.
- McCann HC, Rikkerink EHA, Bertels F, Fiers M, Lu A, Rees-George J, Andersen MT, Gleave AP, Haubold B, Wohlers MW *et al.* 2013. Genomic analysis of the kiwifruit pathogen *Pseudomonas syringae* pv. *actinidiae* provides insight into the origins of an emergent plant disease. *PLoS Pathogens* 9: e1003503.
- Mesarich CH, Rees-George J, Gardner PP, Ghomi FA, Gerth ML, Andersen MT, Rikkerink EHA, Fineran PC, Templeton MD. 2017. Transposon insertion libraries for the characterization of mutants from the kiwifruit pathogen *Pseudomonas syringae* pv. *actinidiae*. *PLoS ONE* 12: e0172790.
- Munkvold KR, Russell AB, Kvitko BH, Collmer A. 2009. *Pseudomonas syringae* pv. *tomato* DC3000 type III effector HopAA1-1 functions redundantly with chlorosis-promoting factor PSPTO4723 to produce bacterial speck lesions in host tomato. *Molecular Plant–Microbe Interactions* 22: 1341–1355.
- Ngou BPM, Ahn H-K, Ding P, Jones JDG. 2021. Mutual potentiation of plant immunity by cell-surface and intracellular receptors. *Nature* 592: 110–115.
- Nowell RW, Laue BE, Sharp PM, Green S. 2016. Comparative genomics reveals genes significantly associated with woody hosts in the plant pathogen *Pseudomonas syringae*: adaptation to woody hosts in *Pseudomonas syringae*. *Molecular Plant Pathology* 17: 1409–1424.
- Parra L, Maisonneuve B, Lebeda A, Schut J, Christopoulou M, Jeuken M, McHale L, Truco M-J, Crute I, Michelmore R. 2016. Rationalization of genes for resistance to *Bremia lactucae* in lettuce. *Euphytica* 210: 309–326.
- Prokhorchik M, Choi S, Chung E, Won K, Dangl JL, Sohn KH. 2020. A host target of a bacterial cysteine protease virulence effector plays a key role in convergent evolution of plant innate immune system receptors. *New Phytologist* 225: 1327–1342.
- Rikkerink E. 2018. Pathogens and disease play havoc on the host epiproteome—the “first line of response” role for proteomic changes influenced by disorder. *International Journal of Molecular Sciences* 19: 772.
- Rodríguez-Puerto C, Chakraborty R, Singh R, Rocha-Loyola P, Rojas CM. 2022. The *Pseudomonas syringae* type III effector HopG1 triggers necrotic cell death that is attenuated by AtNHR2B. *Scientific Reports* 12: 5388.
- Roussin-Léveillé C, Lajeunesse G, St-Amand M, Veerapen VP, Silva-Martins G, Nomura K, Brassard S, Bolaji A, He SY, Moffett P. 2022. Evolutionarily conserved bacterial effectors hijack abscisic acid signaling to induce an aqueous environment in the apoplast. *Cell Host & Microbe* 30: 489–501.
- Sawada H, Fujikawa T. 2019. Genetic diversity of *Pseudomonas syringae* pv. *actinidiae*, pathogen of kiwifruit bacterial canker. *Plant Pathology* 68: 1235–1248.
- Stroud EA, EHA R, Jayaraman J, Templeton MD. 2022. Actigard™ induces a defence response to limit *Pseudomonas syringae* pv. *actinidiae* in *Actinidia chinensis* var. *chinensis* ‘Hort16A’ tissue culture plants. *Scientia Horticulturae* 295: 110806.
- Sun X, Greenwood DR, Templeton MD, Libich DS, McGhie TK, Xue B, Yoon M, Cui W, Kirk CA, Jones WT *et al.* 2014. The intrinsically disordered structural platform of the plant defence hub protein RPM1-interacting protein 4 provides insights into its mode of action in the host-pathogen interface and evolution of the nitrate-induced domain protein family. *FEBS Journal* 281: 3955–3979.
- Tampakaki AP. 2014. Commonalities and differences of T3SSs in rhizobia and plant pathogenic bacteria. *Frontiers in Plant Science* 5: 114.
- Templeton MD, Arshed S, Andersen MT, Jayaraman J. 2022. The complete genome sequence of *Pseudomonas syringae* pv. *actinidifoliorum* ICMP 18803. *BioRxiv*. doi: 10.1101/2022.10.03.510724.
- Templeton MD, Warren BA, Andersen MT, Rikkerink EHA, Fineran PC. 2015. Complete DNA sequence of *Pseudomonas syringae* pv. *actinidiae*, the causal agent of kiwifruit bacterial canker disease. *Genome Announcements* 3: e01054-15.
- Thomas WJ, Thireault CA, Kimbrel JA, Chang JH. 2009. Recombineering and stable integration of the *Pseudomonas syringae* pv. *syringae* 61 *hrp/hrc* cluster into the genome of the soil bacterium *Pseudomonas fluorescens* Pf0-1: stable integration of a T3SS-locus into Pf0-1. *The Plant Journal* 60: 919–928.
- Toruño TY, Shen M, Coaker G, Mackey D. 2019. Regulated disorder: posttranslational modifications control the RIN4 plant immune signaling hub. *Molecular Plant–Microbe Interactions* 32: 56–64.
- Vanneste JL, Yu J, Cornish DA, Tanner DJ, Windner R, Chapman JR, Taylor RK, Mackay JF, Dowlut S. 2013. Identification, virulence, and distribution of two biovars of *Pseudomonas syringae* pv. *actinidiae* in New Zealand. *Plant Disease* 97: 708–719.
- Velásquez AC, Huguet-Tapia JC, He SY. 2022. Shared in planta population and transcriptomic features of nonpathogenic members of endophytic phyllosphere microbiota. *Proceedings of the National Academy of Sciences, USA* 119: e2114460119.
- Wei H-L, Chakravarthy S, Mathieu J, Helmann TC, Stodghill P, Swingle B, Martin GB, Collmer A. 2015. *Pseudomonas syringae* pv. *tomato* DC3000 type

- III secretion effector polymutants reveal an interplay between HopAD1 and AvrPtoB. *Cell Host & Microbe* 17: 752–762.
- Wei H-L, Zhang W, Collmer A. 2018. Modular study of the type III effector repertoire in *Pseudomonas syringae* pv. *tomato* DC3000 reveals a matrix of effector interplay in pathogenesis. *Cell Reports* 23: 1630–1638.
- Wilton M, Subramaniam R, Elmore J, Felsensteiner C, Coaker G, Desveaux D. 2010. The type III effector HopF_{2Pto} targets *Arabidopsis* RIN4 protein to promote *Pseudomonas syringae* virulence. *Proceedings of the National Academy of Sciences, USA* 107: 2349–2354.
- Xin X-F, Nomura K, Aung K, Velásquez AC, Yao J, Boutrot F, Chang JH, Zipfel C, He SY. 2016. Bacteria establish an aqueous living space in plants crucial for virulence. *Nature* 539: 524–529.
- Yoon M, Rikkerink EHA. 2020. *Rpa1* mediates an immune response to *avrRpm1Psa* and confers resistance against *Pseudomonas syringae* pv. *actinidiae*. *The Plant Journal* 102: 688–702.
- Yuan M, Jiang Z, Bi G, Nomura K, Liu M, Wang Y, Cai B, Zhou J-M, He SY, Xin X-F. 2021. Pattern-recognition receptors are required for NLR-mediated plant immunity. *Nature* 592: 105–109.
- Zhang J, Li W, Xiang T, Liu Z, Laluk K, Ding X, Zou Y, Gao M, Zhang X, Chen S *et al.* 2010. Receptor-like cytoplasmic kinases integrate signaling from multiple plant immune receptors and are targeted by a *Pseudomonas syringae* effector. *Cell Host & Microbe* 7: 290–301.
- Zhu Q, Zhao F, Yuan J, Long Y, Fan R, Li Z, Zhao Z, Huang L. 2022. Functional analysis and target identification of the type III effector HopAZ1 from *Pseudomonas syringae* pv. *actinidiae*. *Acta Phytopathologica Sinica* 52: 47–60.

Supporting Information

Additional Supporting Information may be found online in the Supporting Information section at the end of the article.

Fig. S1 *Pseudomonas syringae* pv. *actinidiae* biovar 3 (Psa3) V-13 and *P. syringae* pv. *actinidifoliorum* (Pfm) LV-5 share multiple pore-forming effector orthologs.

Fig. S2 Screen of all single and block effector knockout strains.

Fig. S3 Plasmid complementation of *Pseudomonas syringae* pv. *actinidiae* biovar 3 (Psa3) V-13 effectors *hopS2b* and *hopAZ1a*.

Fig. S4 *Pseudomonas syringae* pv. *actinidiae* biovar 3 (Psa3) V-13 carries four PTI-suppressing effectors.

Fig. S5 Loss of four *Pseudomonas syringae* pv. *actinidiae* biovar 3 (Psa3) V-13 virulence-associated effector loci renders Psa3 V-13 nonpathogenic.

Fig. S6 At least two PTI-suppressing effectors are carried by *Pseudomonas syringae* pv. *actinidifoliorum* (Pfm) LV-5.

Fig. S7 Four *Pseudomonas syringae* pv. *actinidiae* biovar 3 (Psa3) V-13 PTI-suppressing extended exchangeable effector locus (xEEL) effectors are unable to complement *P. syringae* pv. *actinidifoliorum* LV-5 virulence.

Fig. S8 Expression of *Pseudomonas syringae* pv. *actinidifoliorum* (Pfm) LV-5 effectors by plasmid complementation in *P. syringae* pv. *actinidiae* biovar 3 (Psa3) V-13 during expression *in vitro*.

Fig. S9 Screen of all *Pseudomonas syringae* pv. *actinidifoliorum* (Pfm) LV-5 unique effectors in *P. syringae* pv. *actinidiae* biovar 3 (Psa3) V-13.

Fig. S10 *Pseudomonas syringae* pv. *actinidiae* biovar 3 (Psa3) V-13 complemented with *P. syringae* pv. *actinidifoliorum* (Pfm) LV-5 avirulence effector *hopE1a* but not *hopA1a* lacks virulence in planta.

Fig. S11 Screen of *Pseudomonas syringae* pv. *actinidifoliorum* (Pfm) LV-5 unique effectors in *P. syringae* pv. *actinidiae* biovar 3 (Psa3) V-13.

Fig. S12 Biolistic transformation reporter eclipse assays for *Pseudomonas syringae* pv. *actinidifoliorum* (Pfm) LV-5 effectors demonstrate hypersensitive response triggered by HopA1a and HopE1a.

Fig. S13 Deletion of both *Pseudomonas syringae* pv. *actinidifoliorum* (Pfm) LV-5 avirulence effectors does not confer increased virulence.

Fig. S14 Expression of *Pseudomonas syringae* pv. *actinidiae* biovar 3 (Psa3) V-13 effectors by plasmid complementation in *P. syringae* pv. *actinidifoliorum* (Pfm) LV-5 during expression *in vitro*.

Fig. S15 Separate effector knockouts in *Pseudomonas syringae* pv. *actinidiae* biovar 3 (Psa3) V-13 for effectors that complement virulence in *P. syringae* pv. *actinidifoliorum* (Pfm) LV-5 demonstrates effector redundancy.

Fig. S16 Alignment of HopF family effectors from Pto, Psa and Pfm identify HopF4a as a nonfunctional effector.

Table S1 *Pseudomonas syringae* pv. *actinidiae* and *P. syringae* pv. *actinidifoliorum* strains used in this study.

Table S2 Primers used in this study.

Table S3 Comparison of *Pseudomonas syringae* pv. *actinidiae* (Psa3) V-13 and *P. syringae* pv. *actinidifoliorum* (Pfm) LV-5 effectors.

Table S4 Psa3 and Pfm effectors examined in this study.

Please note: Wiley is not responsible for the content or functionality of any Supporting Information supplied by the authors. Any queries (other than missing material) should be directed to the *New Phytologist* Central Office.